Traffic Control via Fleets of Connected and Automated Vehicles

Chiara Daini, Maria Laura Delle Monache, Paola Goatin, Antonella Ferrara

Traffic Control via Fleets of Connected and Automated Vehicles

Chiara Daini[1], Maria Laura Delle Monache[2], Paola Goatin[3] and Antonella Ferrara[4]

***Abstract*—The foreseen deployment of Connected and Automated Vehicles (CAVs) on public roads opens the perspective of reducing the social and environmental impacts of traffic congestion using CAVs as optimal control actuators, operating as moving bottlenecks on the surrounding flow. In this paper, we propose three control strategies, based on different levels of cooperation, to improve density dependent traffic performance indexes, such as fuel consumption.**

We rely on a multi-scale approach to model mixed traffic composed of a small fleet of CAVs in the bulk flow. In particular, CAVs are allowed to overtake (if on distinct lanes) or queuing (if on the same lane). Controlling CAVs desired speeds allows to act on the system to minimize the selected cost function. For the proposed control strategies, we apply both global optimization and a Model Predictive Control approach. In particular, we perform numerical tests to investigate how the CAVs number and positions impacts the result, showing that few, optimally chosen vehicles are sufficient to significantly improve the selected performance indexes, even using a decentralized control policy. Simulation results support the attractive perspective of exploiting a very small number of vehicles as endogenous control actuators to regulate traffic flow on road networks, providing a flexible alternative to traditional control methods. Moreover, we compare the impact of the proposed control strategies (decentralized, quasi-decentralized, centralized).

***Index Terms*—Traffic control, autonomous vehicles, multi-scale traffic flow models, PDE-constraint optimal control.**

I. Introduction

THE recent technological advances in connectivity and automation for the automotive industry are transforming the transportation sector and impacting the related socio-economical aspects. In particular, Connected and Automated Vehicles (CAVs), which are expected to dominate the vehicle market in the next future, have raised the interest of researchers for their potential impact on traffic flow, with the aim of improving traffic conditions and safety. Several studies have shown that CAVs can be employed to control the overall traffic to mitigate congestion and improve throughput, with a consequent reduction of pollutant emissions. This has been proved by model based theoretical results [1]–[10], machine learning approaches [11], [12] and real world experiments [13]. All these investigations show that even a small number of automated vehicles among human-driven vehicles can bring benefits to the whole system, by dissipating stop-and-go waves, improving the throughput and reducing traffic flow emissions and consumption. In this perspective, CAV control can offer a valid, flexible and cheap alternative to more traditional traffic management strategies, such as ramp metering and variable speed limits [14]–[18], which require specific infrastructures.

For traffic control applications, the idea of using multi-scale models in the form of systems of strongly coupled differential equations, representing CAVs as moving bottlenecks acting as variable speed limits, was introduced in [6], [19] and [2]. Models consisting of Partial Differential Equations (PDEs), describing the spatio-temporal evolution of bulk traffic, coupled with Ordinary Differential Equations (ODEs) tracking specific vehicles trajectories, were introduced in the literature to describe the impact of some slow moving vehicles, like buses or trucks, on the surrounding traffic flow [20]–[24]. In the targeted control scenario, multi-scale approaches allow to mitigate the curse of dimensionality, which penalizes the control design for microscopic models [25].

In this framework, CAV optimal control strategies have been applied to the speed of single vehicles [2], [6], small fleets [3], [5] or platoons [4], [8], [26] of CAVs, aiming to improve the energy footprint of traffic by either dissipating stop-and-go waves or reducing traffic congestion. A similar goal is tackled by [27] using a different approach based on a data-driven cruise control in a microscopic framework. We remark that, even if some of the above works consider the presence of several CAVs, no one allows overtaking among the controlled moving bottlenecks. To our knowledge, before [28], [29], moving bottleneck overtaking had been introduced only in [30], but for different optimization purposes.

A. Contribution

In this work, following [28], [29], we develop a general simulation environment modeling the interactions of CAVs and human-driven traffic flow, which enables us to study different CAV-based control strategies with the goal of reducing the overall traffic emissions. To this end, we consider CAVs distributed on different lanes, thus being allowed to queue (if on the same lane) or to overtake (if on distinct lanes). We note that, introducing the ability for the CAVs to interact adds a degree of freedom that can be conveniently used to improve the control performance.

This work was partially supported by ERASMUS+/KA1 "NORTH SOUTH TRAINEESHIP" academic year 2020/21

[1] Chiara Daini is with Inria, SyCOMoRES Research Group, Lille, France chiara.daini@inria.fr

[2]Maria Laura Delle Monache is with the Department of Civil and Environmental Engineering, University of California, Berkeley, USA mldellemonache@berkeley.edu

[3]Paola Goatin is with Université Côte d'Azur, Inria, CNRS, LJAD, France paola.goatin@inria.fr

[4]Antonella Ferrara is with Department of Electrical, Computer and Biomedical Engineering, University of Pavia, Pavia, Italy antonella.ferrara@unipv.it

Our main contribution is to propose three levels of cooperative driving, ranging from a centralized control scheme which assumes the complete knowledge of the traffic conditions and the simultaneous control of the CAV fleet trajectories, to a fully decentralized strategy in which each CAV optimizes its speed, depending on traffic conditions but without taking into account the rest of the fleet. At an intermediate level, we consider a realistic compromise assuming that CAVs optimize their trajectories depending on traffic conditions and taking into account the presence of other fleet items within a limited radius. In the numerical tests, we perform both a global optimization on the full time horizon considered, requiring full knowledge of boundary inflow and outflow conditions, and a Model Predictive Control (MPC) approach that could realistically be implemented in practice. Both optimization strategies show that, if CAV positions are suitably chosen, the quasi-decentralized strategy performs as well as the centralized one. Remarkably, for MPC all the proposed control approaches reach the same performances. Moreover, for all strategies, the gain increases with the number of CAVs, but tends to stabilize quickly even for small fleet sizes. This shows that few, optimally placed vehicles suffice to maximize the selected performance index.

B. Outline

The paper is organized as follows. Section II details the modeling framework, providing a mathematical description of the fully coupled PDE-ODE model including bottleneck interactions, and its numerical discretization. Section III formulates the control problem and illustrates the proposed control strategies, while Section IV describes the results of the numerical experiments.

II. Mixed traffic autonomy model

In this section, we present the multi-scale model describing the interaction of a small fleet of Connected and Automated Vehicles with the surrounding traffic flow. Since we assume the CAV penetration rate is small, they can be tracked one by one because of their specific dynamics and for control purposes. However, it is convenient to model the overall traffic flow from a macroscopic point of view, describing the spatio-temporal evolution of the traffic density. Compared to more detailed microscopic approaches, macroscopic models (also called *hydrodynamic* models for their similarity to fluid dynamics equations) results in a very reduced computational cost and simpler calibration of (few) model parameters, especially when considering large road networks. Still, they provide good estimates of traffic performance indexes, such as average travel times, amount of congestion, fuel consumption, etc.

The interaction dynamics between slow moving vehicles and the surrounding bulk traffic has been studied by several authors, see e.g. [2], [20], [22], [23], [31], [32]. Here we extend to several, possibly interacting CAVs, the model proposed in [21] and then developed in [24], [33]. It consists of the classical Lighthill-Whitham-Richards (LWR) [34], [35] first order macroscopic model accounting for the general evolution of the traffic density, coupled with Ordinary Differential Equations (ODEs) describing the CAVs trajectories.

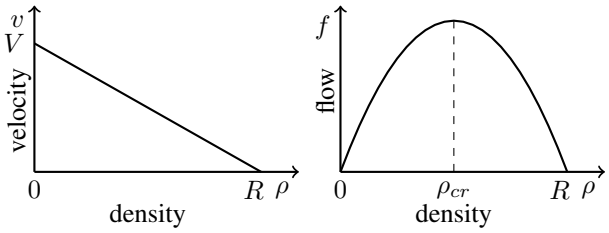

Fig. 1. Greenshields' fundamental diagram.

A. Model definition

To describe the traffic flow on a stretch of highway, we consider the LWR Partial Differential Equation (PDE). This is a *macroscopic first-order* model based on the mass conservation equation:

$$\frac{\partial \rho}{\partial t} + \frac{\partial f(\rho)}{\partial x} = 0,$$

with $x \in \mathbb{R}$ and $t \geq 0$. Above, $\rho = \rho(t,x)$ is the traffic density, defined as the number of vehicles per unit length of the road (veh/km), and $f(\rho) = \rho v(\rho)$ is the flow, defined as the number of vehicles passing the cross-section at location x per unit time (veh/h). The phenomenological speed-density relation $v = v(\rho)$ provides the mean velocity, which is the arithmetic mean speed of the vehicles passing the cross-section per unit time (km/h), as a function of the traffic density.
Several speed laws have been proposed in the literature, see e.g. [36], [37]. For simplicity, we consider here the linear speed function proposed by Greenshields [38]

$$v(\rho) = V\left(1 - \frac{\rho}{R}\right), \tag{1}$$

where V denotes the maximal free flow speed and R the maximal (bump-to-bump) density on the road. The corresponding fundamental diagram is the quadratic function

$$f(\rho) = V\rho\left(1 - \frac{\rho}{R}\right),$$

attaining its maximum at $\rho_{cr} = R/2$ (see Fig. 1). Nevertheless, our study can be extended to any fundamental diagram $f : [0,R] \to \mathbb{R}_+$ with $f(0) = f(R) = 0$, which is concave in the free-flow interval $[0, \rho_{cr}]$.

To account for the presence of CAVs among traffic on a given road segment, we consider the following fully coupled PDE-ODE system:

$$\frac{\partial}{\partial t}\rho\left(t,x\right) + \frac{\partial}{\partial x} f\left(\rho\left(t,x\right)\right) = 0, \tag{2a}$$

$$\dot{y}_\ell(t) = \min\{u_\ell(t), v(\rho(t, y_\ell(t)+))\}, \tag{2b}$$

$$f\left(\rho\left(t, y_\ell(t)\right)\right) - \dot{y}_\ell(t)\rho\left(t, y_\ell(t)\right) \leq \frac{\alpha R}{4V}\left(V - \dot{y}_\ell(t)\right)^2, \tag{2c}$$

together with initial conditions

$$\rho(0,x) = \rho_0(x), \tag{3a}$$

$$y_\ell(0) = y_\ell^0, \tag{3b}$$

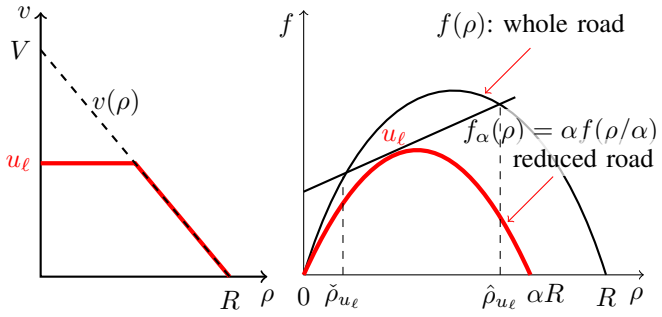

Fig. 2. Left: ℓ-th CAV speed depending on downstream traffic density. Right: reduced flow at ℓ-th CAV position.

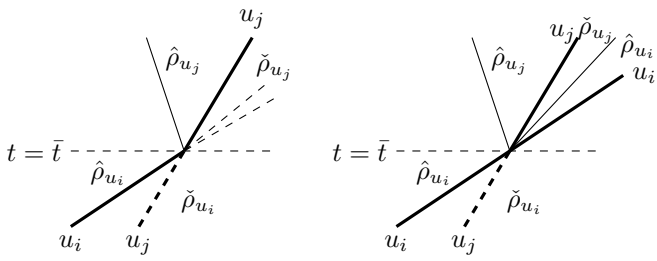

Fig. 3. Examples of interacting CAV trajectories (bold lines). Left: same lane. Right: different lanes.

and boundary conditions

$$f(\rho(t,0)) = f_{in}(t), \tag{4a}$$

$$f(\rho(t,L)) = f_{out}(t). \tag{4b}$$

In (2)-(4), $x \in [0, L]$, $L > 0$ being the length of the considered road segment, $t \in [0, T_f]$, with T_f the time horizon and ρ_0 the initial traffic density on the road. The CAV trajectories are denoted by $y_\ell(t)$, $\ell = 1, \dots, N$, with N the size of the fleet. The CAV desired speeds are the controlled time dependent variables $u_\ell : [0, T_f] \to [0, V]$, $\ell = 1, \dots, N$. Equation (2b) states that each moving bottleneck moves at the prescribed speed $u_\ell(t)$ if the downstream traffic density $\rho(t, y_\ell(t)+)$ allows it. Otherwise, it adapts to the local traffic velocity if it is lower than $u_\ell(t)$ (Fig. 2, left). Besides, the inequalities (2c) account for the moving capacity constraints exerted by CAVs, where $\alpha \in]0, 1[$ is the reduction rate of the road capacity due to the presence of a CAV, which can be set to $\alpha = (M-1)/M$ for all vehicles, where $M \in \mathbb{N}$ is the number of lanes on the road. When active, the constraint induces the formation of a non-classical discontinuity in the traffic density, moving with speed $u_\ell(t)$. The upstream density value is denoted $\hat{\rho}_{u_\ell(t)}$ and downstream density $\check{\rho}_{u_\ell(t)}$ (see Fig. 2, right).

B. Moving Bottlenecks Interactions

To account for interactions between the CAVs, we consider $y_i(\bar{t}) = y_j(\bar{t})$, for some $i, j = 1, \dots, N$, $i \neq j$ and $\bar{t} \in [0, T_f]$. For simplicity, in this work we assume that CAVs stay always in the same lane and are not allowed to change lane to overtake other cars. However, they can overtake other CAVs if they are on different lanes. We can therefore distinguish two situations:

- **Same lane.** If the vehicles are on the same lane, the upstream vehicle travelling with higher speed will adapt to the preceding vehicle and follow it: we get $y_i(t) = y_j(t)$ and $u_i(t) = u_j(t)$ for $t \geq \bar{t}$.
- **Different lanes.** If the vehicles are on different lanes, the faster simply overtakes the slower.

Besides, the constraints (2c) continue to act after the interaction, see Fig. 3. We refer to [29] for a detailed mathematical description of the different interaction dynamics.

C. Model discretization

The approximation scheme used to compute the solutions of the coupled PDE-ODE model (2)-(4) consists of two components: the finite volume discretization of the PDE (2a) with the constraint (2c) and the numerical approximation of the ODEs (2b).

1) Numerical scheme for PDE (2a) *with constraint* (2c)*:* To approximate the constrained LWR model, we use the reconstruction scheme introduced in [39]. It relies on any conservative finite volume scheme for hyperbolic PDEs, coupled with a flux reconstruction technique at the constraint locations. Let Δx and Δt be the fixed space and time steps satisfying the Courant-Friedrichs-Lewy (CFL) condition [40]:

$$V \Delta t = 0.9\, \Delta x,$$

and set $x_{j-1/2} = j\Delta x$, $x_j = (j + 1/2)\Delta x$ for $j = 0, \dots, J$, with $x_{-1/2} = 0$, $x_{J+1/2} = L$, and $t^n = n\Delta t$ for $n = 0, \dots, \lfloor T_f/\Delta t \rfloor$. The algorithm consists of the following steps:

1) Approximate the initial data ρ_0 by piece-wise constant functions $\rho_0^n = \{\rho_{0,j}^n\}_{j=0}^J$ s.t.

$$\rho_{0,j}^n := \frac{1}{\Delta x} \int_{x_{j-1/2}}^{x_{j+1/2}} \rho_0(x)\, dx,$$

for $j = 0, \dots, J$, and boundary data

$$f_{in}^n = \frac{1}{\Delta t} \int_{t^n}^{n+1} f_{in}(t)\, dt,$$
$$f_{out}^n = \frac{1}{\Delta t} \int_{t^n}^{n+1} f_{out}(t)\, dt,$$
$$u_\ell^n = u_\ell(t^n),$$

for $n = 0, \dots, \lfloor T_f/\Delta t \rfloor$.

2) Locate the cell position C_{m_ℓ} of the ℓ-th CAV at time t^n, such that $y_\ell^n \in C_{m_\ell}$, $\ell = 1, \dots, N$.
3) Compute the Godunov numerical fluxes [41] at the cell interfaces $F_{j+\frac{1}{2}}^n = F(\rho_j^n, \rho_{j+1}^n)$, which are given by the supply-demand formula

$$F(\rho_j^n, \rho_{j+1}^n) = \min\{D(\rho_j^n), S(\rho_{j+1}^n)\}, \tag{5}$$

where

$$D(\rho) = f(\min\{\rho, \rho_{cr}\}), \quad S(\rho) = f(\max\{\rho, \rho_{cr}\})$$

(see the Cell Transmission Model [42]).

4) For $\ell = 1, \dots, N$, if the constraint (2c) is not satisfied by the classical Riemann solution corresponding to $\rho^n_{m_\ell - 1}$, $\rho^n_{m_\ell + 1}$, then a moving bottleneck is located at $\bar{x}_{m_\ell} = x_{m_\ell - 1/2} + d^n_{m_\ell}\Delta x \in C_{m_\ell}$ with $d^n_{m_\ell} = \dfrac{\check{\rho}_{u^n_\ell} - \rho^n_{m_\ell}}{\check{\rho}_{u^n_\ell} - \hat{\rho}_{u^n_\ell}}$ and we move to Step 5.
If the constraint (2c) is satisfied, we move to Step 6.
5) If $0 \le d^n_{m_\ell} \le 1$, then
   - Set $\Delta t^n_{m_\ell} = \dfrac{1 - d^n_{m_\ell}}{u^n_\ell}$, Δx.
   - Replace $F^n_{m_\ell - \frac{1}{2}}$ and $F^n_{m_\ell + \frac{1}{2}}$ by
   $F^n_{m_\ell - \frac{1}{2}} = F(\rho^n_{m_\ell - 1}, \hat{\rho}_{u^n_\ell})$ and
   $\Delta t F^n_{m_\ell + \frac{1}{2}} = \min(\Delta t^n_{m_\ell}, \Delta t) f(\check{\rho}_{u^n_\ell}) + \max(\Delta t - \Delta t^n_{m_\ell}, 0) f(\hat{\rho}_{u^n_\ell})$.
6) For $j = 0, \dots, J$, update the density with the conservative formula

$$\rho^{n+1}_j = \rho^n_j - \frac{\Delta t}{\Delta x}\left(F^n_{j+\frac{1}{2}} - F^n_{j-\frac{1}{2}}\right), \tag{6}$$

where the boundary numerical fluxes $F^n_{-\frac{1}{2}}$ and $F^n_{J+\frac{1}{2}}$ are computed setting $D(\rho^n_{-1}) = f^n_{in}$ and $S(\rho^n_{J+1}) = f^n_{out}$ in (5).

Notice that, when they are located in the same cell, the moving bottlenecks are processed sequentially one after the other, first those that are not active (i.e. satisfy (2c)), followed by the active ones (violating (2c)).

2) Numerical scheme for the ODEs (2b)*:* To track the CAV trajectories, at each time step, we update the position y^n_ℓ of the ℓ-th CAV using an explicit Euler scheme: for $\ell = 1, \dots, N$,

- $y^{n+1}_\ell = y^n_\ell + u^n_\ell \Delta t^n$ if the constraint (2c) is not satisfied in step 4) above;
- $y^{n+1}_\ell = y^n_\ell + v(\rho^n_{m_\ell})\Delta t^n$ if (2c) is satisfied.

III. Traffic control problem

In this section, we describe the control strategies applied to the traffic system described above. The control goal is to determine the appropriate CAV velocities, on the basis of the traffic flow conditions, in order to minimize a selected performance index (the *cost function*).

To this end, in this paper we rely on a Model Predictive Control (MPC) approach. MPC is a well-established technique to control dynamical systems, subject to constraints on the state and the control variables, in an optimized way. Following a long history of success in the process industries, in recent years MPC is rapidly expanding in several other domains, such as in the automotive and aerospace industries, smart energy grids, and financial engineering. MPC has also been applied to single-scale (i.e. macroscopic) traffic control, as discussed in [43], [44].

The MPC control algorithm is based on the solution of the optimization problem at each time step of size $\Delta\tau > 0$, taking into account static and dynamic constrains. It is usually implemented relying on the so-called Receding Horizon Control (RHC) concept. This means that, at each time step, the optimal control sequence is determined by solving the optimization problem for the pre-specified prediction horizon $\Delta T > \Delta\tau$; then, only the first sample of the optimal control sequence is applied to the plant and the procedure is repeated at each time step. In this paper, MPC is applied to realize three control solutions that treat the CAVs immersed in the macroscopic traffic differently. They can be classified as centralized, decentralized and quasi-decentralized controls, respectively. In the next sections, we will describe each control strategy separately.

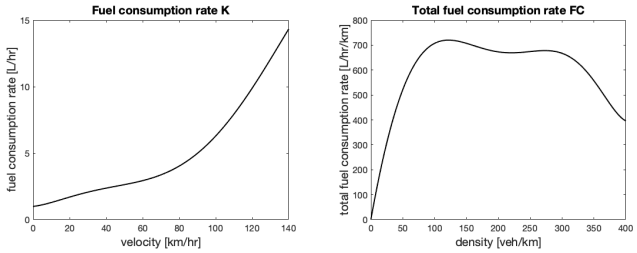

Fig. 4. Plots of the fuel consumption rate function $K(v)$ given by (7) (left) and the corresponding total fuel consumption rate function $FC(\rho) = \rho K(v(\rho))$ (right), given by the speed-density function (1).

A. The cost function

Road transport is one of the main source of air pollution [45]. In particular, vehicular traffic consumption and pollutant emissions are strictly related to the congestion phase, when vehicles accelerate and stop repeatedly [46]. Since in this work we refer to a first order macroscopic model, thus neglecting the traffic acceleration component, we can consider consumption models based on the average speed of vehicles. The cost functional will therefore provide local emission factors, describing average fuel consumption or emissions in kg (or liters) per meter, volume or mass of consumed fuel or emitted pollutant per kilometer and per vehicle [47]. In particular, we will focus on the consumption model derived in [19], which is based on the fuel consumption efficiency data (Liters/km) for four types of vehicles (Ford Explorer, Ford Focus, Honda Civic, and Honda Accord), as functions of the vehicle speed, presented in [48]. Multiplying the fuel consumption efficiency by the vehicle speed yields the fuel consumption rate (Liters/hr). The average fuel consumption rate as a function of the speed derived in [19] is given by

$$\begin{aligned} K(v) = {} & 5.7 \cdot 10^{-12} \cdot v^6 - 3.6 \cdot 10^{-9} \cdot v^5 + 7.6 \cdot 10^{-7} \cdot v^4 \\ & - 6.1 \cdot 10^{-5} \cdot v^3 + 1.9 \cdot 10^{-3} \cdot v^2 + 1.6 \cdot 10^{-2} \cdot v + 0.99, \end{aligned} \tag{7}$$

see Fig. 4, left. Replacing v in (7) by the speed-density law (1), we recover the fuel consumption rate as a function of the traffic density ρ,

$$\widetilde{K}(\rho) = K(v(\rho)), \tag{8}$$

which represents the fuel consumption rate of one vehicles as a function of the traffic density at the vehicle's position. The total fuel consumption rate $FC(\rho)$ is therefore obtained by setting $FC(\rho) = \rho K(v(\rho))$ and is depicted in Fig. 4, right. Lastly, the total fuel consumption of the road stretch $[a, b]$ in the selected time interval $[t_1, t_2]$ is given by:

$$TFC(a, b; t_1, t_2) = \int_{t_1}^{t_2} \int_a^b FC(\rho(t, x))\, dx\, dt. \tag{9}$$

Consider that fuel consumption and greenhouse gas emissions are strictly related: on average, a litre of unleaded petrol produces 2.3 kgs of CO_2. As such, reducing the fuel consumption associated with the overall traffic means correspondingly reducing pollutant emissions [49].

B. Centralized control

Assuming an external controller, a *centralized* control strategy implemented at time $t = \hat{t} \in [0, T_f]$ on a time horizon ΔT takes as input the vector composed by all the controlled CAV positions $y_\ell(\hat{t})$, $\ell = 1, \dots, N$, the current traffic density $\rho(\hat{t}, x)$, $x \in [0, L]$ and the foreseen inflow $f_{in}(t)$ and outflow $f_{out}(t)$, $t \in [\hat{t}, \hat{t} + \Delta T]$, and computes the optimal control $u^* = (u_1^*, \dots, u_N^*) = [\hat{t}, \hat{t} + \Delta T] \to \mathbb{R}^N$ minimizing the selected cost function (here the total fuel consumption $TFC(0, L; \hat{t}, \hat{t} + \Delta T)$). The situation is represented in Fig. 5. In principle, this is the most effective strategy, since the control computation is based on the complete information about the CAVs and the macroscopic traffic state, as well as on the knowledge of the inflow and outflow affecting the traffic system in the considered time horizon.

In an MPC perspective, at the k-th iteration step, we compute the optimal (constant) speed value $u_\ell^*(k)$ for each CAV, $\ell = 1, \dots, N$, taking the current density value $\rho(t_k, \cdot)$ as the initial datum in (3a) over a fixed time horizon $[t_k, t_k + \Delta T]$:

$$u^*(k) = \arg\min TFC(0, L; t_k, t_k + \Delta T), \qquad (10)$$

subject to (2) and the prescribed constraints

$$u_{min} \le u_\ell(k) \le u_{max}, \quad \ell = 1, \dots, N. \qquad (11)$$

We observe that the considered cost functional $TFC(0, L; t_k, t_k + \Delta T)$ is non-linear and non-convex. To avoid local minima, the constrained optimization problem (10)-(11) have been solved using the MATLAB function `fmincon`, a gradient-based method that is designed for non-linear constrained problems, initialized with the optimal velocities computed by `bayesopt`, a Bayesian optimizer which uses a Gaussian process model to minimize the objective function, thus better exploring the admissible control domain. We refer to **Algorithm 1** for an overview of the steps.

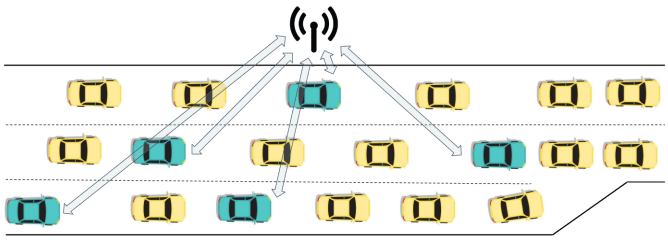

Fig. 5. Schematic representation of the centralized control framework.

C. Decentralized control

Decentralized control strategies aim at controlling a complex multivariable system by decomposing it into simpler subsystems. The latter are controlled by relying only on local information. In the present case, any individual CAV can be regarded as a subsystem. As such, at the k-th iteration step, we compute separately the ℓ-th CAV optimal (constant) speed value $u_\ell^*(k)$, as it were the only controlled vehicle on the road, taking as input the selected CAV position $y_\ell(\hat{t})$, the current traffic density $\rho(\hat{t}, x)$, $x \in [0, L]$ and the foreseen inflow $f_{in}(t)$ and outflow $f_{out}(t)$, $t \in [\hat{t}, \hat{t} + \Delta T]$. For this reason, this control approach can be seen as fully decoupled. The concept is schematized in Fig. 6 and we refer to **Algorithm 2** for an overview of the steps. We notice that, compared to the centralized algorithm, the optimization loop has been inserted in another loop, which splits the different vehicles and processes them separately.

Data: Input initial traffic density ρ_0, CAV positions y_ℓ^0 and velocities $u_\ell(0)$, inflow f_{in} and outflow f_{out}, time horizon T_f, optimization time interval ΔT, simulation time interval $\Delta\tau$
Result: CAV optimal velocities $u_\ell^*(k)$
while $t_k \le T_f$ **do**
  for $t \in [t_k, t_k + \Delta T]$ **do**
    - Solve (10) - (2) with function `bayesopt` for optimal solution $u_{bayes}^*(k) = (u_{1,bayes}^*(k) \dots, u_{N,bayes}^*(k))$
    - Taking as initial point $u_{bayes}^*(k)$, solve (10) - (2) with function `fmincon` for optimal solution $u^*(k) = (u_1^*(k), \dots, u_N^*(k))$
  end
  for $t \in [t_k, t_k + \Delta\tau]$ **do**
    Apply (2) with the optimal solution $u_\ell \leftarrow u_\ell^*(k)$, $\ell = 0, \dots, N$
  end
  $t_k \leftarrow t_k + \Delta\tau$ and update the traffic variables $\rho(t_k, \cdot)$ and $y_\ell(t_k)$, $\ell = 0, \dots, N$
end

Algorithm 1: Centralized control algorithm

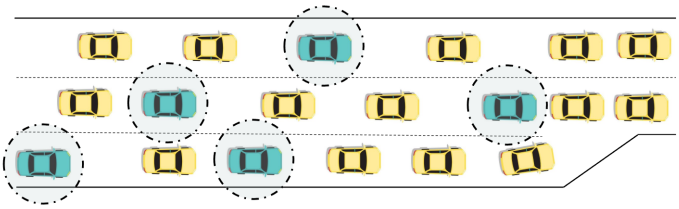

Fig. 6. Schematic representation of the decentralized control framework, where each CAV is treated separately. Its speed is optimized as if it were the only actuator on the road.

D. Quasi-decentralized control

As an intermediate, more viable approach, we consider a partially decentralized control strategy: as in the decentralized control described in Section III-C, we optimize each CAV velocity separately, but considering the system evolution

Data: Input initial traffic density ρ_0, CAV positions y_ℓ^0 and velocities $u_\ell(0)$, inflow f_{in} and outflow f_{out}, time horizon T_f, optimization time interval ΔT, simulation time interval $\Delta\tau$
Result: CAV optimal velocities $u_\ell^*(k)$
while $t_k \leq T_f$ **do**
  for $\ell = 1, \dots, N$ **do**
    Take as inputs $\rho_k(t_k, \cdot)$ and $y_\ell(t_k)$
    for $t \in [t_k, t_k + \Delta T]$ **do**
      - Solve (10) - (2) with function `bayesopt` for optimal solution $u^*_{bayes}(k)$
      - Taking as initial point $u^*_{bayes}(k)$, solve (10) - (2) with function `fmincon` for optimal solution $u^*(k)$

    end
  end
  for $t \in [t_k, t_k + \Delta\tau]$ **do**
    Apply (2) with the optimal solution $u_\ell \leftarrow u_\ell^*(k)$, $\ell = 0, \dots, N$
  end
  $t_k \leftarrow t_k + \Delta\tau$ and update the traffic variables $\rho(t_k, \cdot)$ and $y_\ell(t_k)$, $\ell = 0, \dots, N$
end

Algorithm 2: Decentralized control algorithm

knowing the positions and velocities of the other CAVs in a given radius r, acting as moving bottlenecks. More precisely, for any $l = 1, \dots, N$, let us consider all $m_\ell \in \{1, \dots, N\} \backslash \{\ell\}$ such that

$$|y_{m_\ell}(t_k) - y_\ell(t_k)| \leq r \tag{12}$$

to define the set of ℓ-neighbors $\mathcal{N}_\ell$. We then perform a centralized optimization as in Section III-B, but considering only the CAVs corresponding to the selected neighbor indexes $\mathcal{N}_\ell$, and we keep the optimal velocity u_ℓ^* for the originally selected ℓ-th vehicle.

In Fig. 7, a scheme of the control action is presented. Vehicle A detects other two CAVs within its sensing radius, hence the optimization of its velocity takes into account their presence. On the other hand, vehicle B is too far from other CAVs, thus acting as a fully decentralized controlled vehicle. The optimization procedure is described in **Algorithm 3**.

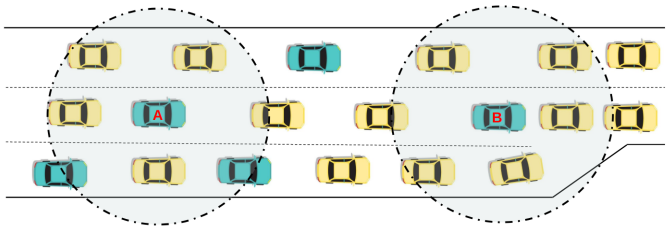

Fig. 7. Schematic representation of the quasi-decentralized control framework.

Data: Input initial traffic density ρ_0, CAV positions y_ℓ^0 and velocities $u_\ell(0)$, inflow f_{in} and outflow f_{out}, time horizon T_f, optimization time interval ΔT, simulation time interval $\Delta\tau$
Result: CAV optimal velocities $u_\ell^*(k)$
while $t_k \leq T_f$ **do**
  for $\ell = 1, \dots, N$ **do**
    $\mathcal{N}_\ell = \emptyset$
    for $m = 1, \dots, N$, **do**
      If (12) holds, $m \in \mathcal{N}_\ell$
    end
    for $t \in [t_k, t_k + \Delta T]$ **do**
      - Solve (10) - (2) with function `bayesOpt` for optimal solutions $u^*_{m,bayes}(k)$, $m \in \mathcal{N}_\ell$
      - Taking as input $u^*_{m,bayes}(k)$, solve (10) - (2) with function `fmincon` for optimal solutions $u^*_m(k)$, $m \in \mathcal{N}_\ell$

    end
  end
  for $t \in [t_k, t_k + \Delta\tau]$ **do**
    Apply (2) with the optimal solution $u_\ell \leftarrow u_\ell^*(k)$, $\ell = 0, \dots, N$
  end
  $t_k \leftarrow t_k + \Delta\tau$ and update the traffic variables $\rho(t_k, \cdot)$ and $y_\ell(t_k)$, $\ell = 1, \dots, N$
end

Algorithm 3: Quasi-decentralized control algorithm

IV. Simulations and Numerical Results

The following tests are aimed at investigating the impact of the different control strategies proposed in Section III. The model framework in which the experiments have been carried out is characterized by a freeway section of length $L = 50$ km with $M = 3$ lanes (corresponding to $\alpha = 0.6$), uniform road conditions with no on- or off-ramps. The maximum speed and maximum density parameters are set to $V = 140$ km/hr and $R = 400$ veh/km, respectively. Considering an average vehicle length of 5 m and a safety distance of 2.5 m, the maximum density is given by [19]:

$$R = \frac{\sharp\text{lanes}}{(2.5 + 5)\ \text{m}} = \frac{3}{7.5\ \text{m}} = 400\ \text{veh/km}. \tag{13}$$

As initial condition, we consider an oscillating density

$$\rho_0(x) = 0.3\, R\, (\sin(0.2\pi x) + 1)\,,$$

mimicking the presence of stop-and-go waves (see Fig. 9, bottom), while the boundary conditions are given by

$$f_{in}(t) = \begin{cases} f_{\max} & \text{if } t \leq 0.5\, T_f, \\ 0 & \text{if } t > 0.5\, T_f, \end{cases} \tag{14}$$

$$f_{out}(t) = 0.5\, f_{\max} \quad \forall t \in [0, T_f], \tag{15}$$

on a time horizon $T_f = 1$ hr, where we have set $f_{\max} = \max_{\rho \in [0,R]} f(\rho) = VR/4 = 14\,000$ veh/hr the capacity of the road. Condition (15) mimics the presence of a fixed bottleneck reducing by half the capacity at the end of the road, due for

example to an accident or construction works, and inducing a backward moving congestion whose effects need to be mitigated.

A. Cost functional sensitivity analysis

To better understand the cost functional considered in (9), we analyze its dependency on constant CAV desired speed $\bar{u} \in [20, 140]$ and initial position $y^0 \in [2, 50]$, considering a single CAV on the road. Fig. 8 represents the TFC as a function of $\bar{u}$ and y^0. The global minimum is close to $\bar{u} = 55$ km/h and $y^0 = 5$ km, while several other local minima are present. In particular, fixing $\bar{u} = 55$ km/h, we observe that the TFC has an increasing trend with respect to the initial position, with local minima located just downstream the higher density regions ($x = 5,\ 15,\ 25,\ 35,\ 45$ km), see Fig. 9. This suggests that vehicles starting farther away from the congestion have a greater impact in reducing the total fuel consumption, subject to local traffic conditions. These local minima are good candidates to be the initial CAV positions in the optimization tests described in Section IV-C.

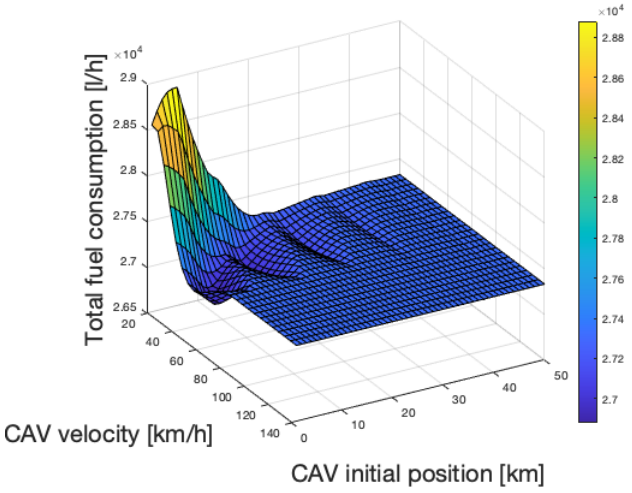

Fig. 8. TFC dependence on the speed $\bar{u} \in [20, 140]$ km/h of a single CAV starting at $y^0 \in [2, 50]$ km.

B. Environment setup

The tests have been realized on fleets of up to $N = 10$ vehicles, distributed on the road starting from the points of local minima observed in Fig. 9; we take $y_1^0 = 5$ km and $y_\ell^0 = y_{\ell-1}^0 + 10$ km, $\ell = 2, \dots, 5$, then $y_6 = 2.5$ km and $y_\ell^0 = y_{\ell-1}^0 + 10$ km, $\ell = 7, \dots, 10$, see Fig. 9, bottom. We assign CAVs sequentially to the different lanes 1 to 3, see Fig. 10.

For each control strategy described in Section III, we implemented the following two setups:

1) **Global optimization** on the whole time interval $[0, T_f]$. Both the optimization horizon ΔT and the simulation interval $\Delta\tau$ are set equal to $T_f = 1$ hr. In this way, only one (global) optimization is performed, to compute the (constant) optimal control values $u^* = (u_1^*, \dots, u_N^*)$. This assumes global knowledge of boundary flow conditions since the initial time $t = 0$.
2) **Model Predictive Control** with $\Delta T = 6$ min and $\Delta\tau = 5$ min. In the perspective of applying this strategy to real environments, the optimization is performed at 4 th minute of the current system evolution interval, to account for the computational time needed to obtain the next control N-tuple. In this way, we guarantee the availability of the newly computed optimal controls for implementation before the end of the current implementation interval.

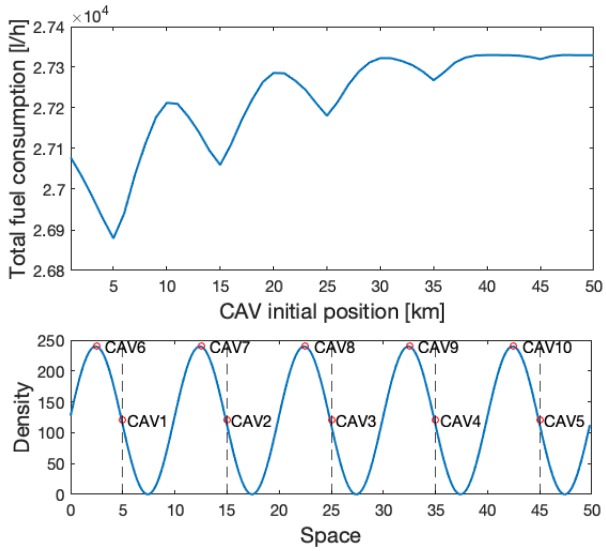

Fig. 9. Top: TFC dependence on the initial position $y^0 \in [2, 50]$ of a single CAV with desired speed $\bar{u} = 55$ km/h. Local minima are located at $x = 5, 15, 25, 35, 45$ km.
Bottom: Initial traffic density ρ_0 and CAV initial positions (dashed lines indicate the location of TFC local minima).

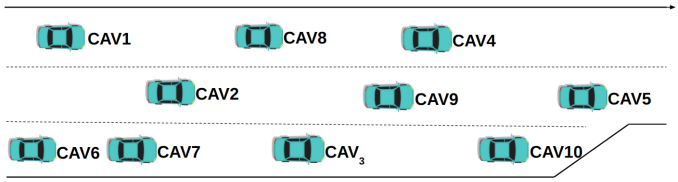

Fig. 10. CAVs' distribution on the road at time $t = 0$.

In all cases, controls will be constrained to the interval $[u_{min}, u_{max}] = [30, 100]$ km/hr, see (11). Moreover, for the quasi-decentralized strategy, we fix the radius $r = 11$ km in (12), aiming at including at least the preceding and following CAVs.

For each control, the comparison will be made with the *uncontrolled* case, where no CAV acts on the traffic flow, see Fig. 11. In this case, the total fuel consumption is $TFC = 2.7329 \cdot 10^4$ liters.

Notice that, because of the computational costs of the optimization routines, in particular for large fleet sizes, we do not compute time-dependent optimal controls, but we limit our study to optimal velocities which are constant in the optimization horizon ΔT. Further efforts are needed to optimize and possibly parallelize the simulation code and the

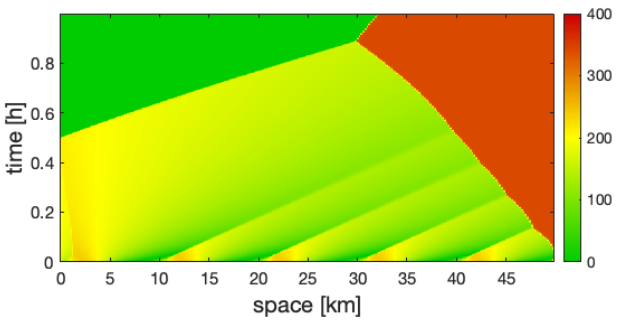

Fig. 11. Spatio-temporal evolution of traffic density in the uncontrolled case.

optimization routines to reduce the overall computational costs of finer optimization procedures.

C. Numerical results

In this section, we present and analyze the results of the performed tests. Fig. 12 reports the trends of the global optimization applied to the centralized, decentralized and quasi-decentralized control strategies. We observe that, for all strategies, the TFC reduction improves for increasing fleet sizes up to 5 vehicles, placed at the optimal positions. Moreover, the quasi-decentralized control is as effective as the centralized one, followed by the fully decentralized. We recall that the centralized control has a global and complete view of the traffic evolution, hence it can compute simultaneously the optimal velocities of all CAVs in the fleet. Instead, the fully decentralized control strategy shows the worst results, because each optimizer/actuator ignores the presence and action of the others CAVs. Placing the vehicles at optimal positions, the quasi-decentralized control reaches the same performance as the centralized, despite having an overview of the traffic flow only locally around each controlled vehicle. We remark that, in this configuration, adding more than five vehicles doesn't diminish the fuel consumption. The curves drawn in Fig. 12 are polynomial interpolations of the computed discrete TFC values, meant to capture the TFC trend as a function of the CAV fleet size. Table I displays the total fuel consumption and its reduction rate with respect to the non-controlled dynamics, for each control strategy applied with $N = 1$, 5, 10 CAVs.

	TFC 1 hour opt. [liters/h]	TFC reduction %
Uncontrolled	$2.7329 \cdot 10^4$	0
1 CAV - centralized	$2.6318 \cdot 10^4$	3.69
1 CAV - decentralized	$2.6319 \cdot 10^4$	3.69
1 CAV - quasi-decentralized	$2.6319 \cdot 10^4$	3.69
5 CAVs - centralized	$2.5650 \cdot 10^4$	6.14
5 CAVs - decentralized	$2.5922 \cdot 10^4$	5.14
5 CAVs - quasi-decentralized	$2.5657 \cdot 10^4$	6.11
10 CAVs - centralized	$2.5687 \cdot 10^4$	6.101
10 CAVs - decentralized	$2.6020 \cdot 10^4$	4.79
10 CAVs - quasi-decentralized	$2.5660 \cdot 10^4$	6.11

TABLE I
1 HOUR OPTIMIZATION TFC VALUES AND GAINS FOR DIFFERENT CAV FLEET SIZES, FOR THE THREE CONTROL STRATEGIES.

On the other hand, Fig. 13 plots the results of MPC optimization corresponding to the three control strategies. Even if the gain is obviously smaller, the trends are similar to the global optimization output reported in Fig. 12: all the strategies improve when increasing the fleet size up to five vehicles, while adding more vehicles in this case seems to deteriorate the result. We notice that with MPC the performances of the three control strategies are practically the same, indicating that the simpler fully decentralized control can be applied as standard procedure. The TFC values and the reduction rates for $N = 1$, 5, 10, are reported in Table II.

	TFC with MPC [liters/h]	TFC reduction %
Uncontrolled	$2.7329 \cdot 10^4$	0
1 CAV - centralized	$2.6933 \cdot 10^4$	1.44
1 CAV - decentralized	$2.6934 \cdot 10^4$	1.44
1 CAV - quasi-decentralized	$2.6978 \cdot 10^4$	1.28
5 CAVs - centralized	$2.6285 \cdot 10^4$	3.82
5 CAVs - decentralized	$2.6314 \cdot 10^4$	3.71
5 CAVs - quasi-decentralized	$2.6320 \cdot 10^4$	3.69
10 CAVs - centralized	$2.6431 \cdot 10^4$	3.29
10 CAVs - decentralized	$2.6507 \cdot 10^4$	3.01
10 CAVs - quasi-decentralized	$2.6346 \cdot 10^4$	3.30

TABLE II
MPC TFC VALUES AND GAINS FOR DIFFERENT CAV FLEET SIZES, FOR THE THREE CONTROL STRATEGIES.

In Figure 14, we show two examples of the space-time traffic density evolution and the corresponding optimal CAV trajectories for a fleet of $N = 10$ vehicles following the quasi-decentralized strategy for 1 hour optimization and MPC, respectively. The red area corresponds to the congestion induced by the downstream bottleneck, while orange zones are local slowdowns generated by the presence of CAVs, which act as moving variable speed limits, delaying upstream flow in reaching the congestion. In particular, we can observe both overtaking and queuing among CAVs, before they reach the congested zone where they all run at the same speed as the sourrounding traffic.

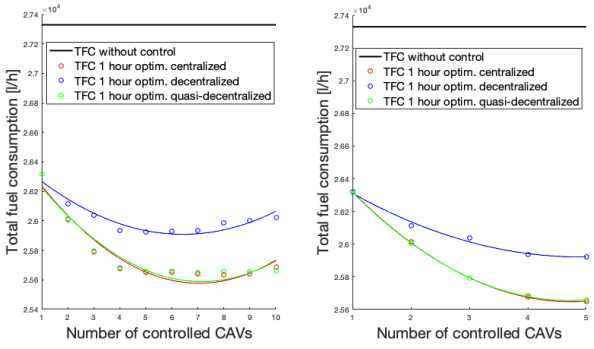

Fig. 12. TFC values resulting form 1 hour global optimization, depending on the number of controlled vehicles: comparison between the different control strategies proposed in Section III.

V. CONCLUSIONS

In this work, we propose three strategies for traffic flow control, which rely on the use of small fleets of Connected and

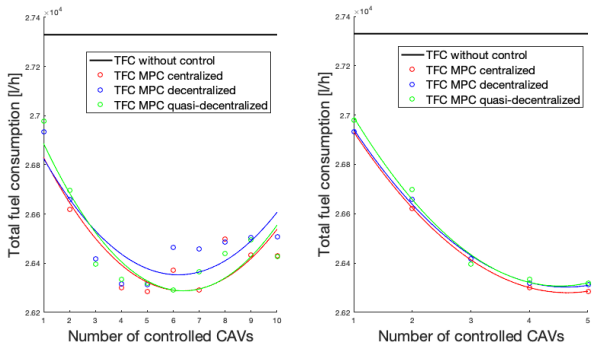

Fig. 13. TFC values resulting form MPC optimization, depending on the number of controlled vehicles: comparison between the different control strategies proposed in Section III.

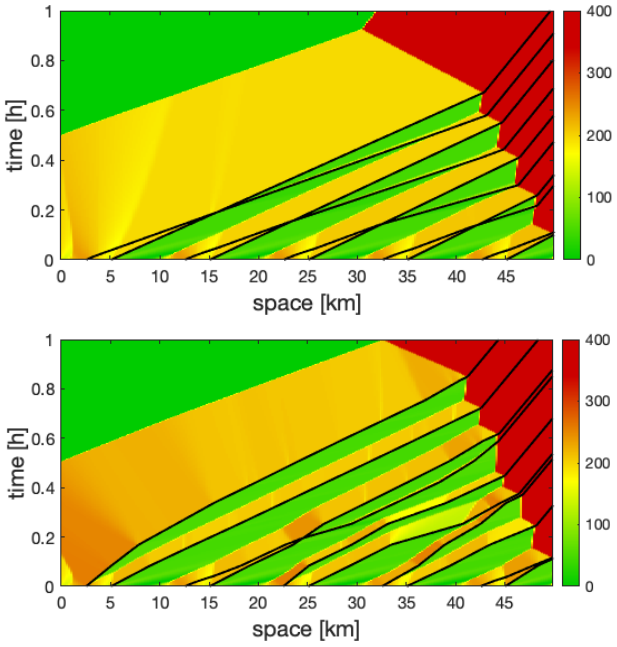

Fig. 14. Traffic density and CAVs trajectories for the quasi-decentralized strategy with a fleet of 10 CAVs and radius $r = 11$ km: 1 hour (top) and MPC (bottom) optimizations.

Automated Vehicles as actuators, corresponding to different levels of cooperation: centralized, decentralized and quasi-decentralized. We show that a small number of well placed CAVs suffices to consistently reduce the fuel consumption of the entire flow and hence to decrease the pollutant emission. The proposed multi-scale modeling approach is numerically efficient and general enough to allow for CAV interactions (overtaking and queuing), and the optimization procedures (global and MPC based) can be applied to improve any traffic index dependent on aggregated traffic quantities (density, mean velocity, flow). Our results support the perspective of testing and validating CAV based cooperative traffic control strategies in real scenarios.

Possible improvements could be offered by further investigation on CAV optimal number and placement depending on traffic conditions. Also, second order models could be employed to better capture some traffic characteristics that would allow to consider a wider class of cost functionals, possibly depending on traffic acceleration.

REFERENCES

[1] A. Talebpour and H. S. Mahmassani, "Influence of connected and autonomous vehicles on traffic flow stability and throughput," *Transportation Research Part C: Emerging Technologies*, vol. 71, pp. 143–163, 2016. [Online]. Available: https://www.sciencedirect.com/science/article/pii/S0968090X16301140

[2] M. Čičić and K. H. Johansson, "Traffic regulation via individually controlled automated vehicles: a cell transmission model approach," in *2018 21st International Conference on Intelligent Transportation Systems (ITSC)*, 2018, pp. 766–771.

[3] ——, "Stop-and-go wave dissipation using accumulated controlled moving bottlenecks in multi-class CTM framework," in *2019 IEEE 58th Conference on Decision and Control (CDC)*, 2019, pp. 3146–3151.

[4] ——, "Energy-optimal platoon catch-up in moving bottleneck framework," in *2019 18th European Control Conference (ECC)*, 2019, pp. 3674–3679.

[5] M. Čičić, I. Mikolášek, and K. H. Johansson, "Front tracking transition system model with controlled moving bottlenecks and probabilistic traffic breakdowns," *IFAC-PapersOnLine*, vol. 53, no. 2, pp. 14 990–14 996, 2020, 21st IFAC World Congress. [Online]. Available: https://www.sciencedirect.com/science/article/pii/S2405896320326288

[6] G. Piacentini, P. Goatin, and A. Ferrara, "Traffic control via moving bottleneck of coordinated vehicles," *IFAC-PapersOnLine*, vol. 51, no. 9, pp. 13–18, 2018.

[7] C. Pasquale, S. Sacone, S. Siri, and A. Ferrara, "A new micro-macro METANET model for platoon control in freeway traffic networks," in *2018 21st International Conference on Intelligent Transportation Systems (ITSC)*, 2018, pp. 1481–1486.

[8] G. Piacentini, P. Goatin, and A. Ferrara, "Traffic control via platoons of intelligent vehicles for saving fuel consumption in freeway systems," *IEEE Control Syst. Lett.*, vol. 5, no. 2, pp. 593–598, 2021.

[9] A. Ferrara, G. P. Incremona, E. Birliba, and P. Goatin, "Multi-scale model based hierarchical control of freeway traffic via platoons of connected and automated vehicles," *IEEE Open Journal of Intelligent Transportation Systems*, pp. 1–1, 2022.

[10] T. Liard, R. E. Stern, and M. L. Delle Monache, "A PDE-ODE model for traffic control with autonomous vehicles," *Networks and Heterogenous Media*, 5 2022. [Online]. Available: https://hal.archives-ouvertes.fr/hal-02492796/document

[11] A. R. Kreidieh, C. Wu, and A. M. Bayen, "Dissipating stop-and-go waves in closed and open networks via deep reinforcement learning," in *2018 21st International Conference on Intelligent Transportation Systems (ITSC)*, 2018, pp. 1475–1480.

[12] E. Vinitsky, K. Parvate, A. Kreidieh, C. Wu, and A. Bayen, "Lagrangian control through deep-rl: Applications to bottleneck decongestion," in *2018 21st International Conference on Intelligent Transportation Systems (ITSC)*, 2018, pp. 759–765.

[13] R. E. Stern, S. Cui, M. L. D. Monache, R. Bhadani, M. Bunting, M. Churchill, N. Hamilton, R. Haulcy, H. Pohlmann, F. Wu, B. Piccoli, B. Seibold, J. Sprinkle, and D. B. Work, "Dissipation of stop-and-go waves via control of autonomous vehicles: Field experiments," *Transportation Research Part C: Emerging Technologies*, vol. 89, pp. 205–221, 2018. [Online]. Available: https://doi.org/10.1016/j.trc.2018.02.005

[14] M. Papageorgiou and A. Kotsialos, "Freeway ramp metering: an overview," *IEEE Transactions on Intelligent Transportation Systems*, vol. 3, no. 4, pp. 271–281, 2002.

[15] A. Hegyi, B. D. Schutter, and J. Hellendoorn, "Optimal coordination of variable speed limits to suppress shock waves," *IEEE Transactions on Intelligent Transportation Systems*, vol. 6, no. 1, pp. 102–112, 2005.

[16] J. Reilly, S. Samaranayake, M. L. Delle Monache, W. Krichene, P. Goatin, and A. M. Bayen, "Adjoint-based optimization on a network of discretized scalar conservation laws with applications to coordinated ramp metering," *J. Optim. Theory Appl.*, vol. 167, no. 2, pp. 733–760, 2015. [Online]. Available: https://doi.org/10.1007/s10957-015-0749-1

[17] P. Goatin, S. Göttlich, and O. Kolb, "Speed limit and ramp meter control for traffic flow networks," *Eng. Optim.*, vol. 48, no. 7, pp. 1121–1144, 2016. [Online]. Available: https://doi.org/10.1080/0305215X.2015.1097099

[18] M. L. Delle Monache, B. Piccoli, and F. Rossi, "Traffic regulation via controlled speed limit," *SIAM Journal on Control and Optimization*, vol. 55, no. 5, pp. 2936–2958, 2017.
[19] R. A. Ramadan and B. Seibold, "Traffic flow control and fuel consumption reduction via moving bottlenecks," 2017, preprint, https://arxiv.org/pdf/1702.07995.pdf.
[20] C. G. Claudel and A. M. Bayen, "Lax–Hopf Based Incorporation of Internal Boundary Conditions Into Hamilton-Jacobi Equation. Part II: Computational Methods," *IEEE Transactions on Automatic Control*, vol. 55, no. 5, pp. 1158–1174, 2010.
[21] J. Lebacque, J. Lesort, and F. Giorgi, "Introducing buses into first-order macroscopic traffic flow models," *Transportation Research Record*, vol. 1644, no. 1, pp. 70–79, 1998. [Online]. Available: https://doi.org/10.3141/1644-08
[22] L. Leclercq, S. Chanut, and J.-B. Lesort, "Moving bottlenecks in Lighthill-Whitham-Richards model: A unified theory," *Transportation Research Record*, vol. 1883, no. 1, pp. 3–13, 2004. [Online]. Available: https://doi.org/10.3141/1883-01
[23] C. Lattanzio, A. Maurizi, and B. Piccoli, "Moving bottlenecks in car traffic flow: a PDE-ODE coupled model," *SIAM J. Math. Anal.*, vol. 43, no. 1, pp. 50–67, 2011. [Online]. Available: https://doi.org/10.1137/090767224
[24] M. L. Delle Monache and P. Goatin, "Scalar conservation laws with moving constraints arising in traffic flow modeling: an existence result," *J. Differential Equations*, vol. 257, no. 11, pp. 4015–4029, 2014. [Online]. Available: https://doi.org/10.1016/j.jde.2014.07.014
[25] M. L. Delle Monache, T. Liard, A. Rat, R. Stern, R. Bhadani, B. Seibold, J. Sprinkle, D. B. Work, and B. Piccoli, *Feedback Control Algorithms for the Dissipation of Traffic Waves with Autonomous Vehicles*. Cham: Springer International Publishing, 2019, pp. 275–299. [Online]. Available: https://doi.org/10.1007/978-3-030-25446-9_12
[26] M. Čičić, L. Jin, and K. H. Johansson, "Coordinating vehicle platoons for highway bottleneck decongestion and throughput improvement," 2020.
[27] J. Wang, Y. Zheng, Q. Xu, and K. Li, "Data-driven predictive control for connected and autonomous vehicles in mixed traffic," in *2022 American Control Conference (ACC)*, 2022, pp. 4739–4745.
[28] C. Daini, P. Goatin, M. L. D. Monache, and A. Ferrara, "Centralized traffic control via small fleets of connected and automated vehicles," in *2022 European Control Conference (ECC)*, 2022, pp. 371–376.
[29] P. Goatin, C. Daini, M. L. Delle Monache, and A. Ferrara, "Interacting moving bottlenecks in traffic flow," *Netw. Heterog. Media*, vol. 18, no. 2, pp. 930–945, 2023. [Online]. Available: https://www.aimspress.com/article/doi/10.3934/nhm.2023040
[30] M. D. Simoni and C. G. Claudel, "A fast simulation algorithm for multiple moving bottlenecks and applications in urban freight traffic management," *Transportation Research Part B: Methodological*, vol. 104, pp. 238–255, 2017. [Online]. Available: https://www.sciencedirect.com/science/article/pii/S0191261517300802
[31] C. F. Daganzo and J. A. Laval, "On the numerical treatment of moving bottlenecks," *Transportation Research Part B: Methodological*, vol. 39, no. 1, pp. 31–46, 2005. [Online]. Available: https://www.sciencedirect.com/science/article/pii/S0191261504000190
[32] R. Borsche, R. M. Colombo, and M. Garavello, "Mixed systems: ODEs - balance laws," *J. Differential Equations*, vol. 252, no. 3, pp. 2311–2338, 2012. [Online]. Available: https://doi.org/10.1016/j.jde.2011.08.051
[33] M. Garavello, P. Goatin, T. Liard, and B. Piccoli, "A multiscale model for traffic regulation via autonomous vehicles," *J. Differential Equations*, vol. 269, no. 7, pp. 6088–6124, 2020. [Online]. Available: https://doi.org/10.1016/j.jde.2020.04.031
[34] M. J. Lighthill and G. B. Whitham, "On kinematic waves. II. A theory of traffic flow on long crowded roads," *Prc. Roy. Soc. London Ser A*, vol. 229, pp. 317–346, 1955.
[35] P. Richards, "Shockwaves on the highway," *Operations Research*, vol. 4, pp. 42–51, 1956.
[36] H. Greenberg, "An analysis of traffic flow," *Operations Research*, vol. 7, no. 1, pp. 79–85, 1959. [Online]. Available: http://www.jstor.org/stable/167595
[37] R. T. Underwood, "Speed, volume and density relationships," *Quality and theory of traffic flow*, 1961.
[38] B. Greenshields, J. Bibbins, W. Channing, and H. Miller, "A study of traffic capacity," in *Highway research board proceedings*, vol. 1935. National Research Council (USA), Highway Research Board, 1935.
[39] C. Chalons, M. L. Delle Monache, and P. Goatin, "A conservative scheme for non-classical solutions to a strongly coupled PDE-ODE problem," *Interfaces and Free Boundaries*, vol. 19, no. 4, pp. 553–570, 2017.
[40] R. Courant, K. Friedrichs, and H. Lewy, "On the partial difference equations of mathematical physics," *IBM journal of Research and Development*, vol. 11, no. 2, pp. 215–234, 1967.
[41] S. Godunov, "A finite difference method for the computation of discontinuous solutions of the equations of fluid dynamics." *Sbornik: Mathematics*, vol. 47, no. 8-9, pp. 357–393, 1959.
[42] C. Daganzo, "The cell transmission model. Part I: A simple dynamic representation of highway traffic. Berkeley, CA: Institute of Transportation Studies," *University of California, Berkeley*, 1993.
[43] S. Siri, C. Pasquale, S. a. Sacone, and A. Ferrara, "Freeway Traffic Control: a Survey," *Automatica*, vol. 130, 2021.
[44] A. Ferrara, S. Sacone, and S. Siri, *Freeway Traffic Modelling and Control*, Springer, Ed., 2018.
[45] C. Pasquale, S. Sacone, S. Siri, and A. Ferrara, "Traffic control for freeway networks with sustainability-related objectives: Review and future challenges," *Annual Reviews in Control*, vol. 48, pp. 312–324, 2019.
[46] S. Kumar Pathak, V. Sood, Y. Singh, and S. Channiwala, "Real world vehicle emissions: Their correlation with driving parameters," *Transportation Research Part D: Transport and Environment*, vol. 44, pp. 157–176, 2016.
[47] M. Treiber and A. Kesting, *Traffic Flow Dynamics*, Springer, Ed., 2013.
[48] I. Berry, "The effects of driving style and vehicle performance on the real-world fuel consumption of U.S. light-duty vehicles." *MIT MS Thesis*, 2010.
[49] U.S. Environmental Protection Agency, "Transportation, air pollution, and climate change," https://www.epa.gov/transportation-air-pollution-and-climate-change.

VI. Biography Section

Chiara Daini received the M.Sc. degree in Industrial Automation Engineering from University of Pavia (Italy) in 2021. In 2021, she completed her M.Sc.'s internship at Inria in Sophia Antipolis (France) in ACUMES team, on traffic control using a macroscopic traffic flow models. She's currently a PhD student at Inria, Lille (France), in SyCoMoRES (Symbolic analysis and Component-based design for Modular Real-Time Embedded Systems) team. Her research interests include real time embedded systems, artificial intelligent optimisation in real time, heterogeneous architectures.

Maria Laura Delle Monache is an assistant professor in the Department of Civil and Environmental Engineering at the University of California, Berkeley. Prior to joining the faculty at UC Berkeley she was a research scientist at Inria in Grenoble, France (2016-2021) and a Postdoctoral fellow at Rutgers University - Camden in USA (2014-2016). She received the B.Sc. degree from the university of L'Aquila (Italy), a joint M.Sc. degree from the University of L'Aquila (Italy) and the University of Hamburg (Germany), and the Ph.D. degree in applied mathematics from the University of Nice-Sophia Antipolis, France in 2009, 2011, and 2014, respectively. She is a member of the Standing Committee on Traffic Flow Theory and Characteristics of the Transportation Research Board and a member of the IEEE Technical Committee on Smart Cities. Dr. Delle Monache's research lies at the intersection of transportation engineering, mathematics and control.

Paola Goatin received the M.Sc. degree in mathematics from University of Padua (Italy) in 1995, the Ph.D. in Applied Mathematics from SISSA-ISAS (Trieste, Italy) in 2000 and the Habilitation in Mathematics from Toulon University in 2009. She is currently Senior Researcher at the Inria Centre of Université Côte d'Azur (France) and leader of the project-team ACUMES (Analysis and Control of Unsteady Models for Engineering Sciences), joint with the mathematics department at Université Côte d'Azur. Before joining Inria in 2010, she held an Applied Mathematics Associate Professorship at Toulon University. Her research interests include: hyperbolic systems of conservation laws, finite volume numerical schemes, macroscopic traffic flow models and PDE-constrained optimization. From 2010 to 2016 she held an ERC Starting Grant on "Traffic Management by Macroscopic models". In 2014, she was awarded the Inria - French Science Academy prize for young researchers. She is author of a hundred publications, including more than 70 journal papers and 1 monograph. She is also member of the Editorial Boards of *SIAM Journal on Applied Mathematics*, *ESAIM: Mathematical Modelling and Numerical Analysis* and *Networks and Heterogeneous Media*.

Antonella Ferrara (S'86, M'88, SM'03, F'20) received the M.Sc. degree in electronic engineering and the Ph.D. degree in computer science and electronics from the University of Genoa, Italy, in 1987 and 1992, respectively. Since 2005, she has been Full Professor of automatic control at the University of Pavia, Italy. Her main research interests include sliding mode control and other nonlinear control methodologies applied to traffic systems, intelligent vehicles, power networks, and robotics. She is author and co-author of more than 450 publications including more than 160 journal papers, 2 monographs and one edited book. At present, she is Senior Editor of the *IEEE Open Journal of Intelligent Transportation Systems* and Associate Editor of *Automatica*. She was Senior Editor of the *IEEE Transactions on Intelligent Vehicles*, Associate Editor of the *IEEE Transactions on Control Systems Technology*, *IEEE Transactions on Automatic Control*, *IEEE Control Systems Magazine*, and *International Journal of Robust and Nonlinear Control*. Dr. Ferrara has been the EUCA Conference Editorial Board Chair since 2018. She is a member of the *IEEE Intelligent Transportation Systems Society* and of the *IEEE Control Systems Society*. She is member of several Technical Committees among which the IEEE TC on Automotive Control, IEEE TC on Smart Cities, IEEE TC on Variable Structure Systems, IFAC Technical Committee on Nonlinear Control Systems, IFAC TC on Transportation Systems, and IFAC Technical Committee on Intelligent Autonomous Vehicles. She is IEEE Fellow and IFAC Fellow.